Role of Ar^{2+} and Ar_2^+ ions in a direct current argon glow discharge: A numerical description

Annemie Bogaerts[a] and Renaat Gijbels
Department of Chemistry, University of Antwerp (UIA), Universiteitsplein 1, B-2610 Wilrijk-Antwerp, Belgium

(Received 8 April 1999; accepted for publication 15 July 1999)

A two-dimensional model has been developed for calculating the behavior of Ar^{2+} and Ar_2^+ ions in a direct current argon glow discharge, by the use of balance equations describing the various production and loss processes for these species, as well as their transport by diffusion and migration. These balance equations are coupled to the equations for the Ar^+ ions and electrons and solved simultaneously with Poisson's equation, to obtain a self-consistent description of the charged particles behavior and the electrical characteristics in the glow discharge. Moreover, this model is combined with the other models that we have developed previously for the Ar atoms in various excited levels and the Cu atomic and ionic species, to obtain an overall description of the direct current argon glow discharge. The model is applied to typical conditions used for glow discharge mass spectrometry (pressure of 50–100 Pa, voltage of 600–1400 V, and current of 0.4–15 mA). Typical calculation results include the densities and fluxes of these ionic species, as well as the relative contributions of their production and loss processes. The Ar^{2+} ions are almost exclusively formed by two-electron ionization from Ar^0 atoms, and they become primarily lost by diffusion and subsequent recombination at the cell walls. The Ar_2^+ ions are mainly created by Hornbeck–Molnar and metastable-metastable associative ionization, whereas atom to molecule conversion seems to play only a minor role at the discharge conditions under study. Loss of these Ar_2^+ ions is caused primarily by diffusion and recombination at the cell walls, but dissociative recombination in the plasma plays also a significant role. We found that the ratios of Ar^{2+}/Ar^+ and Ar_2^+/Ar^+ ion densities and fluxes were in the order of 1%–10%, which is in good agreement with experimental observations. © *1999 American Institute of Physics.* [S0021-8979(99)07920-7]

I. INTRODUCTION

Glow discharges are used in various application fields: in the semiconductor industry for plasma etching and deposition, for lighting and laser purposes, for plasma display panels, in analytical chemistry as spectroscopic source for the analysis of solid materials, etc. In order to improve the results in these applications, a good insight in the glow discharge processes is desirable. We try to obtain this by numerical modeling. In recent years, we have developed a three-dimensional modeling network for various species present in a glow discharge used for analytical applications.[1–9] In this case, the cathode is constructed from the material to be analyzed, and the latter is sputtered by the plasma species. The sputtered, analytically important atoms arrive in the glow discharge plasma, and can be detected, after ionization, by mass spectrometry, or after excitation and subsequent radiative decay, by optical emission spectrometry. The typical working conditions in an analytical glow discharge are voltages around 1000 V, pressures in the order of 0.5–10 Torr, and currents between 1 and 100 mA, in a typical cell of $\sim$1 cm^3 volume, with argon as the discharge gas. However, the model we have developed is also valid for other application fields with similar operating conditions.

The species assumed to be present in the plasma are thermal argon gas atoms, argon ions, fast argon atoms created due to charge transfer and momentum transfer collisions of the argon ions, electrons, argon atoms in various excited levels, sputtered atoms from the cathode material, and the corresponding ions of the cathode material, both in the ground state and in various excited levels. For the argon ionic species, only Ar^+ ions were considered up till now. However, in a typical mass spectrum taken from the analytical glow discharge, also Ar_2^+ ions and Ar^{2+} ions are observed,[10] with relative peak heights about one or two orders of magnitude lower than the Ar^+ peak intensities.[11,12] In order to investigate the role of these species in the glow discharge, we have extended our modeling network to the calculation of the behavior of the Ar^{2+} and Ar_2^+ ions by means of balance equations with various production and loss terms. We are not aware of similar models in the literature for Ar^{2+} ions in glow discharges. For Ar_2^+ ions, some balance equation models have been presented in the literature (e.g., Refs. 13–18), mainly in connection to excimer lasers. However, the latter operate at much higher pressures and the contributions of various production and loss processes can be completely different from our conditions.

II. DESCRIPTION OF THE MODEL

A. General information

The modeling network consists of Monte Carlo, fluid, and collisional-radiative models for the various plasma species mentioned above. Argon was assumed as the discharge

[a]Corresponding author; electronic mail: bogaerts@uia.ua.ac.be

TABLE I. Reaction processes determining the densities of Ar^{2+}, Ar_2^+, Ar^+ ions and electrons, taken into account in the model, and the corresponding rate coefficients.

Reaction process		Rate coefficient
(1) Electron impact ionization of Ar atoms	$Ar^0+e^-\rightarrow Ar^++2e^-$	$\sigma(E)$; Ref. 21
(2) Two-electron impact ionization of Ar atoms	$Ar^0+e^-\rightarrow Ar^{2+}+3e^-$	$\sigma(E)$; Ref. 21
(3) Electron impact ionization of Ar^+ ions	$Ar^++e^-\rightarrow Ar^{2+}+2e^-$	$\sigma(E)$; Ref. 23
(4) Ar atomic to molecular ion conversion	$Ar^++2Ar^0\rightarrow Ar_2^++Ar^0$	$k=2.7\times10^{-31}$ cm^6 s^{-1} (Ref. 44)
(5) Associative ionization (Hornbeck–Molnar)	$Ar^{**}+Ar^0\rightarrow Ar_2^++e^-$	$k=2\times10^{-9}$ cm^3 s^{-1} (Ref. 34)
(6) Metastable-metastable ionization collisions	$Ar_m^*+Ar_m^*\rightarrow Ar^++Ar^0+e^-$	$k=6.3\times10^{-10}$ cm^3 s^{-1} (Ref. 38)
(7) Metastable-metastable associative ionization	$Ar_m^*+Ar_m^*\rightarrow Ar_2^++e^-$	$k=5.7\times10^{-10}$ cm^3 s^{-1} (Ref. 38)
(8) Ar^+ - electron three body recombination	$Ar^++2e^-\rightarrow Ar^0+e^-$	$k=7\times10^{-27}$ cm^6 s^{-1} (Ref. 24)
(9) Ar^{2+} - electron three body recombination	$Ar^{2+}+2e^-\rightarrow Ar^++e^-$	$k=1.35\times10^{-25}$ cm^6 s^{-1} (Ref. 24)
(10) Ar_2^+ dissociative recombination	$Ar_2^++e^-\rightarrow Ar^0+Ar^0$	$k=8.5\times10^{-7}(T_e/300)^{-0.67}(T_g/300)^{-0.58}$ (Ref. 48)
(11) Penning ionization of sputtered Cu atoms	$Ar_m^*+Cu^0\rightarrow Ar^0+Cu^++e^-$	$k=2.36\times10^{-10}$ cm^3 s^{-1} (Ref. 9)
(12) Asymmetric 1-electron charge transfer	$Ar^++Cu^0\rightarrow Ar^0+Cu^+$	$k=2.36\times10^{-10}$ cm^3 s^{-1} (Ref. 9)
(13) Asymmetric 2-electron charge transfer	$Ar^{2+}+Cu^0\rightarrow Ar^0+Cu^{2+}$	$k=5\times10^{-10}$ cm^3 s^{-1} (Ref. 25)
(14) Fast Ar ion impact ionization of Ar atoms	$Ar^0+Ar_f^+\rightarrow Ar^++Ar^++e^-$	$\sigma(E)$ (Ref. 55)
(15) Fast Ar atom impact ionization of Ar atoms	$Ar^0+Ar_f^0\rightarrow Ar^++Ar^0+e^-$	$\sigma(E)$ (Ref. 55)

Note: Ar_m^* and Ar** denote the Ar metastable $4s$ levels and the Ar highly excited levels (see below), respectively, and the other symbols are straightforward.

gas and copper was taken as the cathode material. Briefly, the fast electrons are described with a Monte Carlo model.[1–3] The slow electrons and the argon (Ar^+) ions are treated in a fluid model;[2,3] the latter incorporates also Poisson's equation, in order to obtain a self-consistent electric field distribution from the electron and ion densities. The argon ions are also followed with a Monte Carlo model in the cathode dark space (CDS) of the glow discharge;[1,4] indeed, this region is characterized by a strong electric field; the ions can gain rather high energies, and are therefore more accurately described in a Monte Carlo model. The fast argon atoms, created from the argon ions by charge transfer and momentum transfer collisions, are also simulated with a Monte Carlo model in the CDS.[1,4] The behavior of the argon atoms in various excited levels, including the metastable levels, is described in a collisional-radiative model;[5] 65 levels were considered; each level was described with a balance equation with various collisional and radiative populating and depopulating processes. The copper atoms, when sputtered from the cathode, are characterized by energies of a few eV; they lose these energies almost immediately by collisions with the argon gas atoms until they are thermalized; this thermalization process is also treated with a Monte Carlo model.[6] The further behavior of the copper atoms, i.e., transport by diffusion, ionization, and excitation, and the behavior of the corresponding copper ions and excited copper atoms and ions, is again simulated with a collisional-radiative model.[7–9] Finally, the copper ions are also described with a Monte Carlo model in the CDS,[7,8] where they can reach rather high energies due to the high electric field. More information about these various models can be found in Refs. 1–9. The present article will be focused on the modeling of the behavior of Ar^{2+} and Ar_2^+ ions, and the incorporation of these calculations in the entire modeling network.

The reaction processes determining the densities of Ar^{2+} and Ar_2^+ ions, as well as the electron and Ar^+ ion densities (which are calculated simultaneously with the Ar^{2+} and Ar_2^+ ions; see Sec. II D), and which are taken into account in our model, are presented in Table I, together with the rate coefficients used (see also Secs. II B and II C).

The calculations are performed at typical operating conditions for glow discharge mass spectrometry (GDMS; voltages around 1000 V, pressures of 0.4–1 Torr, currents of 1–10 mA), and are applied to the standard source for analyzing flat samples in the commercial VG9000 glow discharge mass spectrometer (VG Elemental, Thermo Instruments). A schematic picture of this source is given in Fig. 1.[3] Since this cell has cylindrical symmetry, the three dimensions could be reduced to two dimensions (axial and radial direction).

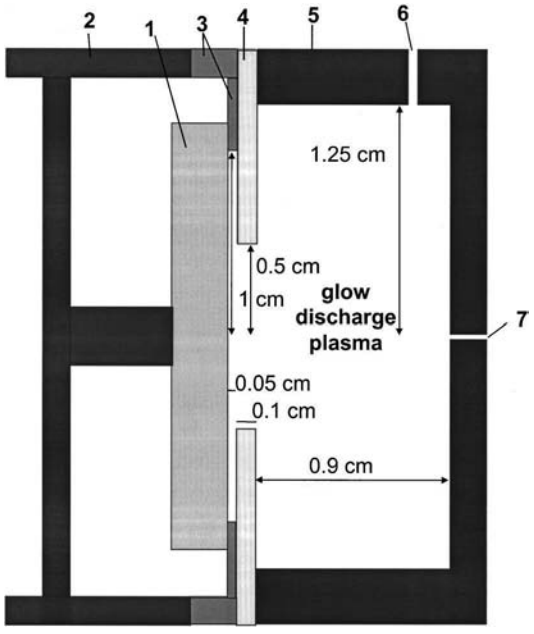

FIG. 1. Schematic picture of the glow discharge cell to be modelled. 1: sample (cathode), 2: sample holder (cathode potential), 3: insulator, 4: front plate (anode potential), 5: cell house (anode potential), 6: gas inlet, 7: exit slit towards mass spectrometer.

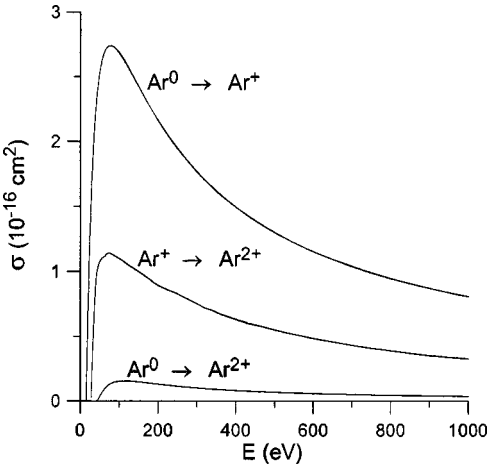

FIG. 2. Cross sections of electron impact ionization for $Ar^0 \rightarrow Ar^+$, $Ar^+ \rightarrow Ar^{2+}$, and $Ar^0 \rightarrow Ar^{2+}$, as a function of the electron energy.

B. Model for the Ar^{2+} ions

The density of the Ar^{2+} ions, as a function of z and r position, is calculated with a balance equation:

$$\frac{\partial n_{Ar^{2+}}(z,r)}{\partial t} + \bar{\nabla}.\bar{j}_{Ar^{2+}}(z,r) = R_{prod}(z,r) - R_{loss}(z,r),$$

where n, j, and R symbolize the number density (cm^{-3}), flux ($cm^{-2}\,s^{-1}$), and production or loss rates ($cm^{-3}\,s^{-1}$) of the Ar^{2+} ions, respectively. The transport of the Ar^{2+} ions is governed by diffusion and by migration in the electric field:

$$\bar{j}_{Ar^{2+}}(z,r) = \mu_{Ar^{2+}} n_{Ar^{2+}}(z,r)\bar{E}(z,r) - D_{Ar^{2+}}\bar{\nabla} n_{Ar^{2+}}(z,r),$$

where μ and D stand for the mobility and diffusion coefficient of Ar^{2+} ions, and E is the electric field distribution. The diffusion coefficient was assumed to be equal to the one for Ar^+ ions [i.e., taken as 100 $cm^2\,s^{-1}$ at 1 Torr (Ref. 2)]. The mobility was adopted from Ref. 19. Data were given as a function of the electric field over gas density ratio (E/n), in the range of 40–200 Td. We are, however, interested in higher E/n values as well. Indeed, in the CDS, the electric field is usually in the order of 1000–10 000 V/cm; for a typical gas density of $10^{16}\,cm^{-3}$, this yields $E/n \sim 10^{-13}$–$10^{-12}\,V\,cm^2$ or 10–100 kTd (since 1 Td $=10^{-17}\,V\,cm^2$). Therefore, we fitted a curve through the data of Ref. 19, similar to the Frost formula for Ar^+ ions,[20] which we used for higher E/n values also:

$$\mu = \frac{\mu_0}{\sqrt{1 + a(E/n)}},$$

where μ_0 is 2192.4 $cm^2\,V^{-1}\,s^{-1}$ at 1 Torr, and a is 2.83×10^{14}.

The production processes taken into account for the Ar^{2+} ions are electron impact ionization from the Ar^0 gas atoms [Table I, reaction (2)] and from the Ar^+ ions [reaction (3)]. The cross section for the first process is adopted from Ref. 21, where a fit was made to the experimental data of Stephan *et al.*[22] The cross section of the second process was found in Ref. 23. Both cross sections are plotted as a function of the electron energy in Fig. 2, as well as, for comparison, the cross section of electron impact ionization for $Ar^0 \rightarrow Ar^+$, which was also taken from Ref. 21. The cross section for $Ar^+ \rightarrow Ar^{2+}$ is a factor of 2–2.5 lower than the one for $Ar^0 \rightarrow Ar^+$, whereas the $Ar^0 \rightarrow Ar^{2+}$ cross section is still almost one order of magnitude lower than the $Ar^+ \rightarrow Ar^{2+}$ value. However, since the Ar^0 atom density is four to five orders of magnitude higher than the Ar^+ ion density,[2,3] we expect that reaction (2) is still more important than reaction (3). The cross sections as a function of the electron energy for reactions (2) and (3) have been included in the electron Monte Carlo model developed previously,[1–3] and the corresponding reaction rates calculated with this model are used as input values for the production term of the above balance equation.

The loss processes incorporated in this balance equation are electron-ion three-body recombination to Ar^+ [reaction (9)] and two-electron asymmetric charge transfer with Cu^0 atoms [reaction (13)] which is a resonant process (i.e., good energy overlap between the ion and atom energy levels). The rate constant for the first loss process is taken from Ref. 24, where the values for He and Sr are given. This rate constant depends on the distribution of the energy levels, e.g., for He the excited levels lie close to the ionization limit, whereas for Sr and the other alkali elements, the excited levels are more evenly distributed. Since Ar also has excited levels close to the ionization limit, we adopted the same value as for He. Moreover, the formulas for this three-body electron-ion recombination process given in this article contain a factor: $Z^3 \ln\sqrt{Z^2+1}$, where Z is the charge of the ion. Hence, this formula can be used for multiply charged ions as well. For Ar^+ ions ($Z=1$), this factor is 0.3466, whereas for Ar^{2+} ions ($Z=2$), this factor amounts to 6.4378, hence, a factor of 18.575 higher. Therefore, the rate constant for electron—Ar^{2+} recombination was derived to be: $k = 3.55 \times 10^{14} T_e^{-11}\,cm^6\,s^{-1}$ for $T_e > 3100$ K. If T_e is assumed to be 5000 K,[9] this yields $k = 1.351 \times 10^{-25}\,cm^6\,s^{-1}$. Finally, the rate constant for the two-electron asymmetric charge transfer with Cu^0 atoms was assumed to be $5 \times 10^{-10}\,cm^3\,s^{-1}$, based on the cross section value given in Ref. 25.

The boundary condition for this balance equation is $\partial n/\partial x = 0$ at all walls, similar to the Ar^+ ion boundary condition.

C. Model for the Ar_2^+ ions

The Ar_2^+ ions are described with a similar balance equation, which also yields the flux and density as a function of z and r position:

$$\frac{\partial n_{Ar_2^+}(z,r)}{\partial t} + \bar{\nabla}.\bar{j}_{Ar_2^+}(z,r) = R_{prod}(z,r) - R_{loss}(z,r),$$

where n, j, and R symbolize again the number density (cm^{-3}), flux ($cm^{-2}\,s^{-1}$), and production or loss rates ($cm^{-3}\,s^{-1}$) of the Ar_2^+ ions, respectively. The transport of the Ar_2^+ ions occurs again by diffusion and by migration in the electric field:

$$\bar{j}_{(Ar_2^+)}(z,r) = \mu_{(Ar_2^+)} n_{(Ar_2^+)}(z,r)\bar{E}(z,r) - D_{(Ar_2^+)}\bar{\nabla} n_{(Ar_2^+)}(z,r),$$

where μ and D stand again for the mobility and diffusion coefficient, respectively; and E is the electric field strength. The value of the mobility was found to be 1.83 $cm^2 s^{-1} V^{-1}$ at 760 Torr and 273 K, remaining more or less constant as a function of E/n.[19] Hence, we adopted this value as a constant in our calculations. Further, we assumed that the diffusion coefficient was half the value of Ar^+ ions, based on an inverse proportionality with the ion mass.

The production of Ar_2^+ ions is caused by associative ionization, i.e., both by collisions of two metastable Ar_m^* atoms [reaction (7)] and by the collision of a highly excited Ar** atom with a ground state Ar atom [the so-called Hornbeck–Molnar process; reaction (5)], as well as by atomic ion to molecular ion conversion [reaction (4)]. The loss of Ar_2^+ ions is assumed to occur entirely due to dissociative recombination [reaction (10)], which is known to be much more efficient than other (e.g., three-body) recombination processes.[27] In principle, other production and loss processes can also determine the density of Ar_2^+ ions (see, e.g., Refs. 13,14,18,26), but they involve species like Ar_2^* and Ar_3^+, which are not included in our model, because they are expected to become only significant at high pressures.[18]

Data for these production and loss processes were not always easy to find. The Hornbeck–Molnar process has been investigated by many authors (e.g., Refs. 28–37), but most of these papers give only qualitative evidence of the importance of this process. In Ref. 34, however, rate constants of 1.3×10^{-9}, 1.7×10^{-9}, and 2×10^{-9} $cm^3 s^{-1}$ have been found for three different excited Ar** levels. These values are high but realistic in view of the collision diameters.[34] In the early paper of Pahl,[30] the value of 2×10^{-9} $cm^3 s^{-1}$ was already suggested. This value was also considered realistic in Ref. 36, since it yields a radiative lifetime in satisfactory agreement with measured values. Therefore, we adopted this value of 2×10^{-9} $cm^3 s^{-1}$ for our calculations. Furthermore, although some previous works[33,34] revealed only three excited Ar** states which give rise to this process, in Ref. 35 over 20 states were identified to yield this process, and ionization was observed at every absorption line of shorter wavelength than the threshold of 14.71 eV. Therefore, we can assume that all excited Ar** levels, with energies higher than 14.71 eV, which is the ionization potential of Ar_2 to form Ar_2^+ ions, can give rise to this process. The populations of the Ar excited levels were calculated in our previously developed collisional-radiative model for Ar, with takes into account 65 levels.[5] Some of these levels were considered separately, like the four $4s$ metastable and resonant levels, whereas the higher excited levels were combined into effective levels. Figure 3 shows the populations of these levels at the maximum of their two-dimensional profiles, as a function of the effective level number n, calculated for the cell shown in Fig. 1, at 75 Pa, 1000 V, and 4.2 mA. The statistical weights corresponding to these effective levels are also indicated on the figure. Based on the threshold of 14.71 eV, it appears that the Hornbeck–Molnar associative ionization is possible for the Ar** $4d$ and $6s$ levels, and all higher levels, which corresponds in the model to effective level number $n=20$ and higher (see Ref. 5 for more details). It should be mentioned that this process was not incorporated in our collisional-radiative model before.[5] It appears, however, to be a very important loss process for these highly excited levels. Hence, the presently calculated level populations of the effective levels with $n\geqslant20$ have decreased by a factor of 3–7 compared to Ref. 5.

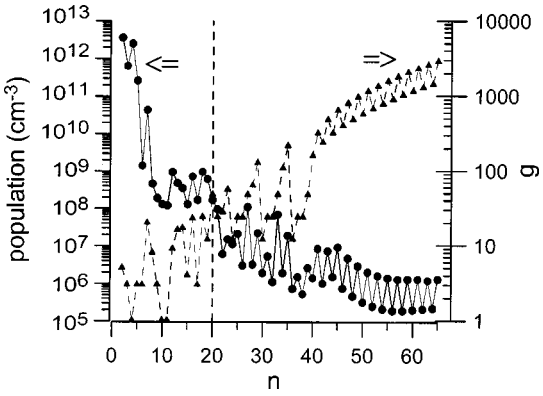

FIG. 3. Level populations of the Ar excited levels as a function of the effective level number n, calculated with our Ar* collisional-radiative model (see Ref. 5) (solid line, left axis) as well as the statistical weight of these effective levels (dashed line, right axis).

The data for associative ionization due to the collisions of two metastable Ar_m^* atoms were even more difficult to find. Most often, the rate coefficients are given for the general reaction between two Ar_m^* atoms, but this can also lead to the formation of Ar^+. In Ref. 38 a value of 1.2×10^{-9} $cm^3 s^{-1}$ was found for the ionization reaction between two Ar $4s\,^3P_2$ levels. Furthermore, in Ref. 16 it was reported that the rate constant for formation of Ar_2^+ was 0.9 times the value for formation of Ar^+ ions. Hence, we assumed a value of 6.3×10^{-10} $cm^3 s^{-1}$ for formation of Ar^+ and a value of 0.9 times this number, i.e., 5.7×10^{-10} $cm^3 s^{-1}$, for creation of Ar_2^+. The latter value is in excellent agreement with the value suggested by Neeser[14] for this reaction process (i.e., 6×10^{-10} $cm^3 s^{-1}$). Although the rate constant of 1.2×10^{-9} $cm^3 s^{-1}$ was only measured for the collision between 2 Ar_m^* atoms in the $^3P_2$ levels,[38] we assumed the same value for collisions between all four $4s$ Ar_m^* (metastable and resonance) levels. The populations of these $4s$ levels were also calculated in our collisional-radiative model for Ar excited levels,[5] and the level populations at the maximum of their profiles are also presented in Fig. 3.

The rate coefficient for atomic to molecular ion conversion was easier to find in the literature (e.g., Refs. 13–15,18,39–45). The values were all more or less consistent with each other (i.e., ranging between 1.9×10^{-31} and 4.7×10^{-31} $cm^6 s^{-1}$), so that they are expected to be more or less reliable. We used the following value:[44] $k_{conv}=2.7\times10^{-31}$ $cm^6 s^{-1}$. It should be mentioned that this rate coefficient applies actually only to Ar^+ ions in the $^2P_{3/2}$ level.[44] The corresponding rate coefficient for the Ar^+ ions in the $^2P_{1/2}$ level was reported to be much lower, i.e., 2×10^{-32} $cm^6 s^{-1}$ as an upper limit.[44] We assume that, based on the statistical weights, about 2/3 of the Ar^+ ions will be in the $^2P_{3/2}$ level, and about 1/3 is in the $^2P_{1/2}$ level, and the

populations of excited Ar^+ ion levels are much lower. Hence, only 2/3 of the Ar^+ ions is assumed to react in the atomic to molecular ion conversion, with the above mentioned reaction rate; and the reaction process with the Ar^+ ions in the $^2P_{1/2}$ level is neglected.

The rate coefficient for dissociative recombination was also reported in a number of papers (e.g., Refs. 46–49), and the values were all more or less in agreement with each other. We adopted the value of Ref. 48, i.e., $k_{\text{dis.recom.}} = 8.5 \times 10^{-7}(T_e/300)^{-0.67}(T_g/300)^{-0.58}$.

Finally, the boundary condition for this balance equation is similar to the one for Ar^+ and Ar^{2+} ions, i.e., $\partial n/\partial x = 0$ at all walls (see above and Ref. 2).

D. Implementation of this Ar^{2+} and Ar_2^+ model in the entire modeling network

The balance equations for the Ar^{2+} and Ar_2^+ ions are included in our fluid model for the Ar^+ ions and slow electrons,[2,3] because some of the production and loss processes of these ions can also affect the Ar^+ ion and electron densities. Indeed, atomic to molecular ion conversion from Ar^+ to Ar_2^+ and electron impact ionization from Ar^+ to Ar^{2+} are additional loss processes for the Ar^+ ions, whereas electron-Ar^{2+} recombination is an addition production process for the Ar^+ ions. Moreover, the electrons can become lost not only due to recombination with Ar^+ ions, but also with Ar_2^+ and Ar^{2+} ions. Finally, the Ar^{2+} and Ar_2^+ ions contribute to the space charge, and together with the affected Ar^+ ion and electron densities they will determine the potential distribution via Poisson's equation. Therefore, the balance equations of Ar^{2+} and Ar_2^+ ions are coupled to the equations for Ar^+ ions and electrons, and to the Poisson equation, and they are solved like in Refs. 2,3, based on the Scharfetter–Gummel exponential scheme.[50,51]

Moreover, this new fluid model affects also the other models in our existing modeling network. Indeed, the Ar^{2+} and Ar_2^+ ion fluxes bombarding the cathode determine, together with the Ar^+ ion flux, the electron flux due to secondary electron emission. The electrons leaving the cathode by secondary electron emission are then followed in our Monte Carlo model. This effect is especially important for the Ar^{2+} ions, because the secondary electron emission coefficient due to impact of these species is about a factor of 3 higher than for Ar^+ impact.[52] Further, also the other species which play a role in some of the production and loss processes of the Ar^{2+} and Ar_2^+ ions (see Table I), like the highly excited Ar** atoms (process 5), the Ar_m^* metastable atoms (process 7), and the sputtered Cu^0 atoms (process 13), are affected by the present model; and their densities have to be recalculated taking into account the reactions described above.

Figure 4 shows the complete flowchart of the entire modeling network. It is an extension of the flowchart shown e.g., in Refs. 53,54, with the addition of the effect of the Ar^{2+} and Ar_2^+ ions on the other models (presented in bold). Because the various submodels can influence each other, the entire modeling network is solved iteratively, until final convergence is reached.

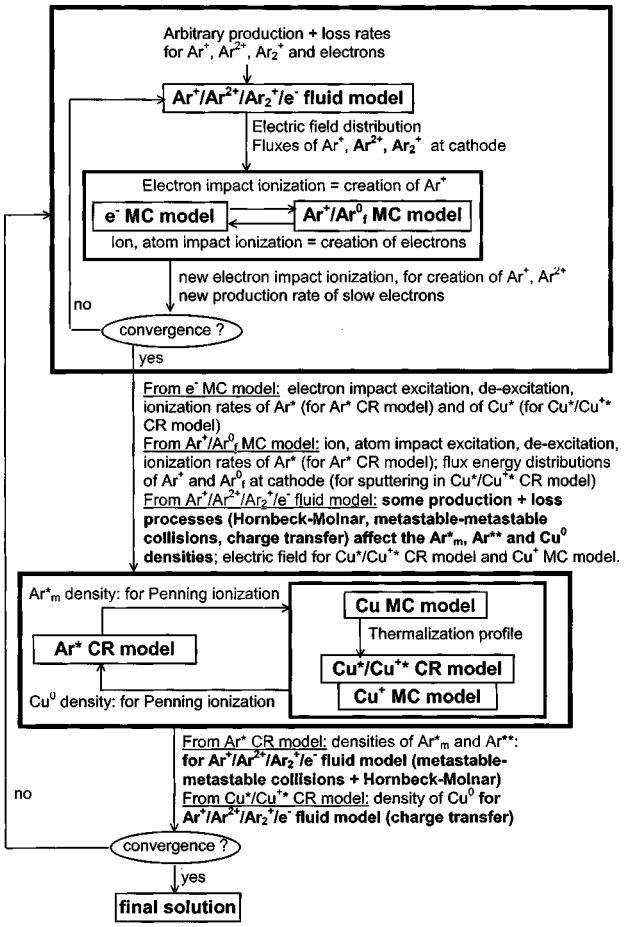

FIG. 4. Flowchart of the entire modeling network, indicating the effect of the Ar^{2+} and Ar_2^+ ions in bold.

III. RESULTS AND DISCUSSION

A. Densities and fluxes

Figure 5(a) presents the two-dimensional density of Ar^{2+} ions in the VG9000 cell, at 75 Pa, 1000 V, and 4.2 mA. The cathode is at the left end of the figure, whereas the other figure borders represent the anode walls. The density is low and rather constant in the cathode dark space (CDS; i.e., the first two mm's, where a strong electric field is present) and reaches a maximum of about $2\times10^{10}\,\text{cm}^{-3}$ at 4–5 mm from the cathode. The density of the Ar_2^+ ions in the same VG9000 cell is depicted in Fig. 5(b). The two-dimensional density profile looks very much the same as the Ar^{2+} ion density profile, both in shape and in absolute value. For comparison, Fig. 5(c) illustrates the Ar^+ ion density in the VG9000 cell. It has the same relative profile, but reaches a maximum of about $6\times10^{11}\,\text{cm}^{-3}$. Hence, the Ar^{2+}/Ar^+ and Ar_2^+/Ar^+ density ratios are about 3%.

The effect of voltage and pressure on the calculated densities of Ar^{2+}, Ar_2^+, and Ar^+ ions, at the maximum of their profiles, is plotted in Figs. 6(a), 6(b), and 6(c), respectively. Figure 6(d) presents the calculated currents, as a function of voltage and pressure, which might be useful to obtain an idea on the effect of current as well. All densities increase with voltage and pressure (and current). The effect on the Ar^{2+}

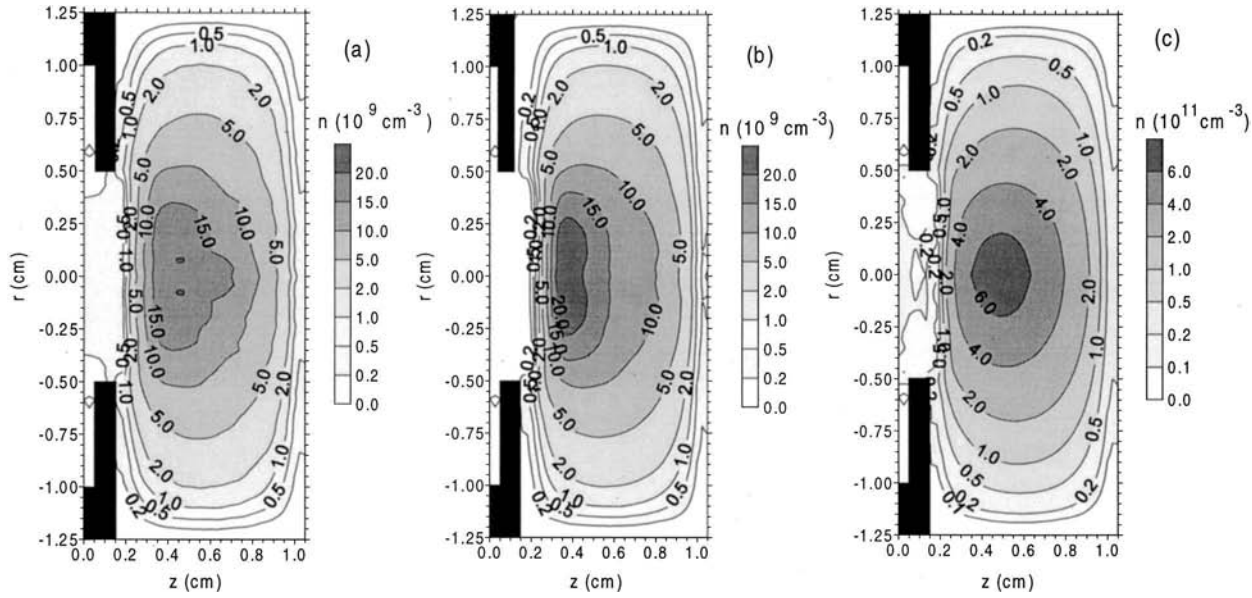

FIG. 5. Calculated two-dimensional density profiles of the (a) Ar^{2+}, (b) Ar_2^+, and (c) Ar^+ ions, in the VG9000 cell, at 75 Pa, 1000 V, and 4.2 mA. The cathode is at the left side of the figure. The black rectangles from $z=0$ to 0.05 cm denote the insulating ring, and the black rectangles from $z=0.05$ to 0.15 cm symbolize the front plate at anode potential. The other borders of the figure represent the anode cell walls.

and Ar^+ ions is very similar, but the Ar_2^+ ion density has a somewhat different behavior. Indeed, it increases less rapidly with voltage, but more rapidly with pressure. The reason is that at higher voltages, the production of Ar_2^+ ions increases, but the loss of Ar_2^+ ions, due to electron-ion dissociative recombination increases also (due to the increased electron density), and it tends to balance more or less the increased production. The more pronounced increase with pressure is in agreement with other calculation results, where it is found that the Ar_2^+/Ar^+ density increases as the cube of the pressure.[56] In Ref. 26, for example, it is demonstrated that the Ar_2^+ ions are the dominant ionic species (i.e., density of $\sim 8\times 10^{11}\,cm^{-3}$ compared to $\sim 1.4\times 10^{11}\,cm^{-3}$ for the Ar^+ ion density) in the positive column of a dc glow discharge at 100 Torr and 10.89 mA. Indeed, at these high pressures, atomic to molecular ion conversion (which is still of minor importance at our lower pressures; see below) is a very important production process due to the interaction with two argon atoms, and it is responsible for the rapid increase of the Ar_2^+ density with pressure.

To investigate the role of the Ar^{2+} and Ar_2^+ ions in the overall discharge, the Ar^+ ion densities at the maximum of their profiles, calculated without the incorporation of Ar^{2+} and Ar_2^+ ions in the model, are also depicted in Fig. 6(c) (dashed lines). It appears that the Ar^{2+} and Ar_2^+ ions have a non-negligible effect on the Ar^+ ion density, i.e., the latter increases by about 20%–30% when the description of Ar^{2+} and Ar_2^+ ions is added to the model. The reason for this is not so much the direct effect of processes involving Ar^{2+} and Ar_2^+ ions which yield an increase in the production of Ar^+ ions, but rather the increase in calculated electrical current when Ar^{2+} and Ar_2^+ are taken into account. Indeed, the flux of these Ar species is typically 1%–10% of the Ar^+ ion flux (see below). As mentioned before, especially the Ar^{2+} ions can play an important role, because (i) they carry twice as much electrical current as the other charged species in the model, and more importantly (ii) they give rise to more efficient secondary electron emission at the cathode (their secondary electron emission coefficient is approximately three times higher[52] than for Ar^+); hence, more electrons are emitted from the cathode and can give rise to more ionization in the plasma, increasing again the electrical current.

From the densities at the maximum (Fig. 5), the ratio of Ar^{2+}/Ar^+ and of Ar_2^+/Ar^+ densities can be obtained. The ratio of Ar^{2+}/Ar^+ densities is about 2%–6% for all discharge conditions investigated, whereas the ratio of Ar_2^+/Ar^+ densities decreases from ~8% at low voltage to ~1% at the higher voltages investigated.

We have also calculated the fluxes of these ionic species, and it was found that the ratios of the Ar^{2+}/Ar^+ and Ar_2^+/Ar^+ ion fluxes are very similar to the ratios of the densities (i.e., varying between 1% and 10%). This is in good agreement with experimental observations,[11] where the intensity ratios in the mass spectrum (which correspond to the fluxes at the anode backplate of the cell) were measured for various Ar species, at similar discharge conditions. The Ar^{2+} ion intensity was found to be about 10% of the Ar^+ ion intensity, whereas the Ar_2^+/Ar^+ ion intensity ratio was about 2%–4%, as can be seen in Fig. 7. Hence, although the agreement is not yet perfect, the calculated results seem to be in the correct order of magnitude. The latter is not straightforward, taking into account the large uncertainties in the collision rate constants and cross sections, and the fact that these Ar species have not been studied before in such detail for our conditions. It appears also from Fig. 7 that the Ar^{3+} and Ar_3^+ ions are characterized by much lower intensities, and that these species can hence be neglected at our model conditions.

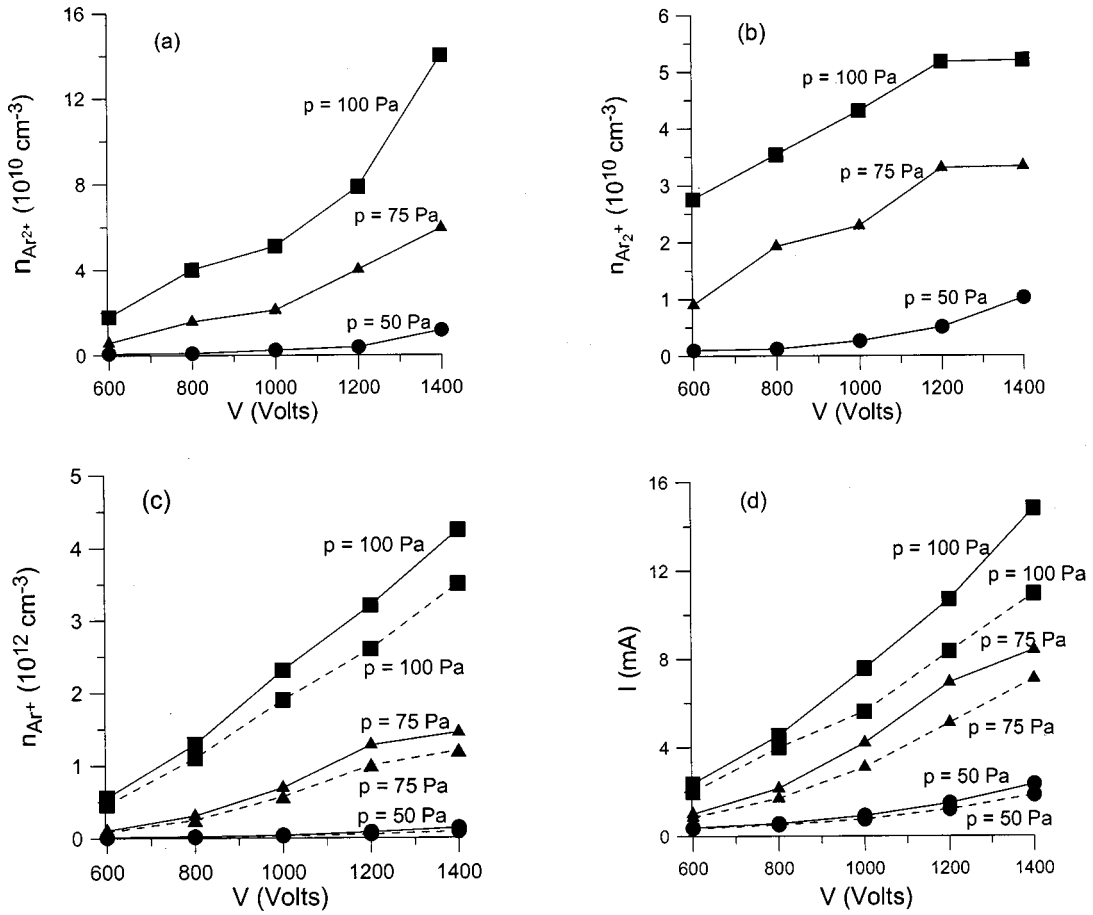

FIG. 6. Calculated (a) Ar^{2+}, (b) Ar_2^+, and (c) Ar^+ densities at the maxima of the profiles, as well as (d) the calculated electrical currents, all as a function of voltage and pressure. The solid and the dashed lines in (c) and (d) illustrate the calculated quantities with and without the incorporation of the Ar^{2+} and Ar_2^+ ions in the model, respectively.

B. Production and loss processes

In Table II, the relative contributions of the various production and loss processes of the Ar^{2+} ions and Ar_2^+ ions are presented, for 1000 V, 75 Pa, and 4.2 mA.

As was already anticipated based on the cross sections and the densities of Ar^0 atoms and Ar^+ ions, two-electron ionization from Ar^0 atoms is clearly the dominant production process for the Ar^{2+} ions (99.99%), and one-electron ionization from Ar^+ ions can be neglected (0.01%). This was found to be the case for all the discharge conditions under study. Moreover, the Ar^{2+} ions become almost exclusively lost by diffusion and subsequent recombination at the cell walls (99.5%). Two-electron asymmetric charge transfer is responsible for about 0.5% of the loss, whereas electron-ion recombination is completely negligible. The contribution of charge transfer as a loss mechanism increases slightly with pressure and voltage (up to ~1.7% at the highest voltage and pressure investigated).

The Ar_2^+ ions are primarily formed by associative ionization, both through highly excited Ar** levels (Hornbeck–Molnar: ~57.4%) and by collisions of two Ar metastable atoms (about 41.4%). The remaining 1.2% of the Ar_2^+ ions are created by atomic to molecular ion conversion. The latter process slightly gains importance with increasing pressure (i.e., ~0.3% at 50 Pa, about 1%–1.2% at 75 Pa, and up to a value of about 2.2% at 100 Pa), but it never becomes dominant at the discharge conditions under investigation. The Hornbeck–Molnar process seems to be the most important production process at the discharge conditions under study, but it decreases with increasing voltage, at the expense of metastable-metastable associative ionization, which becomes equally important or even slightly dominant at the highest voltages under study. Hence, it seems that at higher voltages

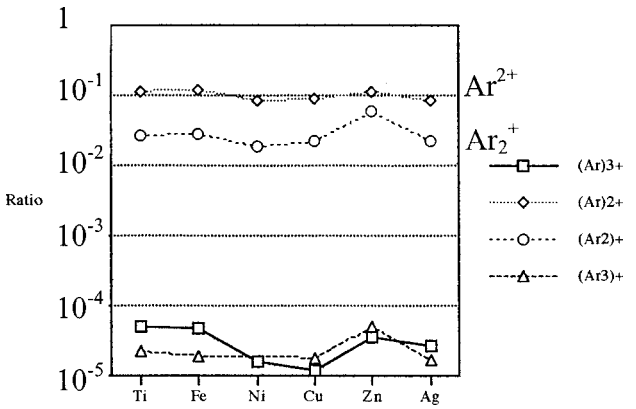

FIG. 7. Measured intensity ratios in the glow discharge mass spectrum for different Ar species relative to Ar^+ ions, for different cathode materials (see Ref. 11).

TABLE II. Relative contributions of the production and loss processes of the Ar^{2+}, Ar_2^+, and Ar^+ ions and electrons, at 75 Pa, 1000 V, and 4.2 mA.

Species	% production	% loss
Ar^{2+}	Two-electron ionization from Ar^0: 99.99	Diffusion: 99.5
	One-electron ionization from Ar^+: 0.01	two-electron charge transfer with Cu: 0.5
		Recombination to Ar^+: 10^{-5}
Ar_2^+	Hornbeck–Molnar assoc.ionization: 57.4	Diffusion: 82.6
	Metastable-metastable assoc.ionization: 41.4	Dissociative recombination: 17.4
	Atom to molecule conversion: 1.2	
Ar^+	Electron impact ionization: 87.4	Diffusion: 99.6
	Fast atom impact ionization: 6.5	Charge transfer with Cu: 0.3
	Fast ion impact ionization: 2.0	Atom to molecule conversion: 0.1
	Metastable-metastable ionization: 4.1	Recombination to Ar^0: 10^{-4}
	Ar^{2+} - electron recombination: 10^{-7}	
Electrons	Electron impact ionization: 79	Diffusion: 98.7
	Fast atom impact ionization: 5.9	Recombination with Ar_2^+: 1.3
	Fast ion impact ionization: 1.8	Recombination with Ar^+: 10^{-4}
	Hornbeck–Molnar assoc.ionization: 4.3	Recombination with Ar^{2+}: 10^{-6}
	Metastable-metastable assoc.ionization: 3.7	
	Metastable-metastable ionization: 3.3	
	Penning ionization: 2.2	

the metastable levels are more populated than the higher excited levels. This is at first sight unexpected, because at the higher voltages, the electrons have higher energy and can more easily populate the higher excited levels. However, it was found in our model[5] that the lower Ar levels (like the $4s$ metastable and resonant levels and the $4p$ levels) can also be populated by fast argon ion and atom impact excitation, and the latter processes become increasingly important at higher voltages. Whether this model observation correctly reflects the real situation still has to be investigated. Hence, the exact relative contributions of both associative ionization processes should be considered with caution, especially because the rate constants are subject to uncertainties (see before). Nevertheless, it is clear from Table II that both processes are clearly more important than atomic to molecular ion conversion at the discharge conditions under investigation. As far as the loss of Ar_2^+ ions is concerned, diffusion and subsequent recombination at the cell walls is again most important (about 82.6%), but the contribution of electron-ion dissociative recombination (calculated to be 17.4%) is certainly not negligible, as was expected already from the rather high rate coefficient (see Table I). Moreover, the latter loss process increases clearly with pressure and also slightly with voltage (i.e., contribution of about 0.3% at 50 Pa and 600 V, and about 33% at 100 Pa and 1400 V), the reason being that the electron density also increases significantly with voltage and pressure. The importance of the latter loss process is responsible for the minor increase of the Ar_2^+ density with increasing voltage (see above).

As discussed before, the Ar^{2+} and Ar_2^+ ions can also affect the Ar^+ ions and electrons, by some production and loss processes. Therefore, the relative contributions of the various production and loss processes of the Ar^+ ions and electrons are also tabulated in Table II. The majority of the Ar^+ ions are formed by electron impact ionization (87.4%). However, fast ion and especially atom impact ionization are not completely negligible (i.e., 2% and 6.5%, respectively). Moreover, ionization due to metastable-metastable collisions also has a contribution of ~4%. The latter three processes become increasingly important at higher voltages (i.e., in the order of 1% at 600 V, rising to almost 10% at 1400 V). The pressure seems to have only a minor effect on these relative contributions. The loss of the Ar^+ ions is again primarily caused by diffusion and recombination at the cell walls (99.6%). Only a small fraction is lost due to asymmetric charge transfer with Cu^0 atoms (0.3%) and due to atom to molecule conversion (0.1%). Electron-ion recombination is still of minor importance (10^{-4}%). This situation is true for all discharge conditions investigated, although the contribution of loss due to charge transfer increases with pressure and voltage (up to 1.7% at 100 Pa and 1400 V), and atom to molecule conversion increases slightly with pressure (i.e., a contribution of ~0.02% at 50 Pa, ~0.1% at 75 Pa, and ~0.2% at 100 Pa).

The electrons are also dominantly formed by electron impact ionization (79%). However, a number of other processes each contribute for a few percent, i.e., fast atom impact ionization (5.9%), fast ion impact ionization (1.8%), Hornbeck–Molnar associative ionization (4.3%), metastable-metastable collisions leading to the formation of Ar^+ (3.7%), and of Ar_2^+ (3.3%) and Penning ionization of the Cu^0 atoms (2.2%). The contributions of all these minor production processes rise slightly with voltage whereas the pressure has only negligible effect. However, electron impact ionization remains always the most significant production process (contribution minimum about 80%). The loss seems to be again primarily due to diffusion and recombination at the walls (98.7%). Recombination in the plasma occurs mainly with the Ar_2^+ ions (around 1.3%), in spite of their lower density compared to the Ar^+ ions. Dissociative recombination is indeed much more efficient compared to electron-ion three-body recombination with Ar^+ or Ar^{2+} ions, which have a contribution in the order of 10^{-4} and 10^{-6}%, respectively. The latter two processes remain negligible at all conditions investigated, but dissociative recombination increases to a contribution of about 3% at 100 Pa and 1400 V.

IV. CONCLUSION

We have calculated the densities and fluxes of the Ar_2^+ and Ar^{2+} ions in a direct current argon glow discharge, by means of two balance equations taking into account the various production and loss processes of these species. These balance equations are coupled to the equations of Ar^+ ions and electrons and to Poisson's equation, to calculate self-consistently the charged particle behavior. Moreover, this two-dimensional model is combined with our other models for the Ar excited levels and the sputtered Cu species, to obtain an overall description of the argon direct current glow discharge.

The model is applied to a typical cell used for glow discharge mass spectrometry, operating at ~1000 V, 50–100 Pa, and a few mA. The results include the densities and fluxes of the ionic species, as well as the relative contributions of the various production and loss processes. The Ar^{2+} densities range from $7\times10^8\,cm^{-3}$ at low pressure and voltage to $\sim1.5\times10^{11}\,cm^{-3}$ at high pressure and voltage. The Ar_2^+ ions were also found to have a density of about $10^9\,cm^{-3}$ at low pressure and voltage; they rise also with pressure, but they do not increase so much with voltage; therefore they reach a maximum of only about $5\times10^{10}\,cm^{-3}$ at the highest voltage and pressure investigated. We have compared these densities with the Ar^+ ion densities, and found that the ratio of Ar^{2+}/Ar^+ ion densities was always around 2%–6%, whereas the ratio of Ar_2^+/Ar^+ ion densities decreases from about 8% at low voltage to ~1% at the highest voltage investigated. The reason for this decreasing importance of the Ar_2^+ ions seems to be the high electron densities in our conditions, and hence the growing importance of the loss by dissociative recombination. The ratios of the fluxes of Ar^{2+}/Ar^+ and Ar_2^+/Ar^+ ions were found to be very similar to the density ratios. These calculated ratios are in satisfactory agreement with experimental observations, where intensity ratios in the mass spectrum (which correspond to calculated ion flux ratios at the anode backplate of the cell) of about 10% were found for Ar^{2+}/Ar^+ and about 2%–4% for Ar_2^+/Ar^+.

As far as the production and loss processes of the various species is concerned, the Ar^{2+} ions are almost exclusively formed by two-electron ionization from Ar^0, and they become mainly lost by diffusion and subsequent recombination at the cell walls. The Ar_2^+ ions are predominantly formed by associative ionization, both through highly excited Ar** atoms (Hornbeck–Molnar process) and by metastable-metastable collisions. Atomic to molecular ion conversion is only of minor importance at the operating conditions under study. Loss of the Ar_2^+ ions occurs mainly by diffusion and recombination at the walls, although dissociative recombination in the plasma is also quite significant.

Finally, the Ar^{2+} ions and Ar_2^+ ions have also some effect on the other calculated plasma quantities. Since the Ar^{2+} ions carry twice as much electrical current as the other charged plasma species, and since they give rise to more efficient secondary electron emission at the cathode, the electrical current has increased by 20%–30% after including the Ar^{2+} and Ar_2^+ ions in our model. Also the Ar^+ ion densities have increased by this amount, due to an increase in the electrical current, and hence in the ionization rate. It was also found that the incorporation of the Hornbeck–Molnar associative ionization to Ar_2^+, caused a drop in the level populations of the higher excited Ar** levels by a factor of 3–7, and that this process should therefore really be included in Ar* collisional-radiative models. Moreover, the Hornbeck–Molnar process, as well as the collisions between two metastable Ar_m^* atoms leading to Ar_2^+ (and to Ar^+) ions contribute each for about 5% to the additional creation of electrons. However, this effect is more or less balanced by the additional loss of electrons due to Ar_2^+ electron dissociative recombination, so that the electron density does not change dramatically (except for some increase due to the increased electrical current; see above). Finally, the two-electron charge transfer process between Ar^{2+} and Cu^0 will increase the density of Cu^{2+} ions.

In general, it can be concluded that the Ar^{2+} and Ar_2^+ ions play some roles in the glow discharge behavior at the operating conditions under study, and that their densities are not negligible. Hence, at the discharge conditions presented here, these species should be included for accurate modeling of the glow discharge behavior.

ACKNOWLEDGMENTS

A. Bogaerts is indebted to the Flemish Fund for Scientific Research (FWO) for financial support. This research is also sponsored by NATO's Scientific Affairs Division in the framework of the Science for Peace Programme, and by the Federal Services for Scientific, Cultural and Technical Affairs of the Prime Minister's Office through IUAP (Conv. P4/10). Finally, the authors would like to thank G. Petrov, N. Sadeghi, R. Carman, B. Peart, and K. Wiesemann for the helpful information.

[1] A. Bogaerts, M. van Straaten, and R. Gijbels, Spectrochim. Acta B **50B**, 179 (1995).
[2] A. Bogaerts, R. Gijbels, and W. J. Goedheer, J. Appl. Phys. **78**, 2233 (1995).
[3] A. Bogaerts, R. Gijbels, and W. J. Goedheer, Anal. Chem. **68**, 2296 (1996).
[4] A. Bogaerts and R. Gijbels, J. Appl. Phys. **78**, 6427 (1995).
[5] A. Bogaerts, R. Gijbels, and J. Vlcek, J. Appl. Phys. **84**, 121 (1998).
[6] A. Bogaerts, M. van Straaten, and R. Gijbels, J. Appl. Phys. **77**, 1868 (1995).
[7] A. Bogaerts and R. Gijbels, J. Appl. Phys. **79**, 1279 (1996).
[8] A. Bogaerts and R. Gijbels, Anal. Chem. **68**, 2676 (1996).
[9] A. Bogaerts, R. Gijbels, and R. Carman, Spectrochim. Acta B **53B**, 1679 (1998).
[10] J. S. Becker, G. Seifert, A. I. Saprykin, and H.-J. Dietze, J. Anal. At. Spectrom. **11**, 643 (1996).
[11] P. Kennis, Ph.D. dissertation, University of Antwerp, 1996.
[12] M. van Straaten, A. Bogaerts, and R. Gijbels, Spectrochim. Acta B **50B**, 583 (1995).
[13] E. Elson and M. Rokni, J. Phys. D **29**, 717 (1996).
[14] S. Neeser, T. Kunz, and H. Langhoff, J. Phys. D **30**, 1489 (1997).
[15] N. Sadeghi-Kharrazi, Ph.D. dissertation, University of Grenoble, 1974.
[16] J. Pavlik, J. Glosik, M. Sicha, M. Tichy, and P. Potocek, Contrib. Plasma Phys. **30**, 437 (1990).
[17] Ts. Petrova, E. Benova, G. Petrov, and I. Zhelyazkov, Phys. Rev. E (submitted).
[18] G. M. Petrov and C. M. Ferreira, Internal Report CFP 10/97, Instituto Superior Technico, Lisbon Technical University.

[19] H. W. Ellis, R. Y. Pai, E. W. McDaniel, E. A. Mason, and L. A. Viehland, At. Data Nucl. Data Tables **17**, 177 (1976).
[20] L. S. Frost, Phys. Rev. **105**, 354 (1957).
[21] R. J. Carman, J. Phys. D **22**, 55 (1989).
[22] K. Stephan, H. Helm, and T. D. Märk, J. Chem. Phys. **73**, 3763 (1980).
[23] K. F. Man, A. C. H. Smith, and M. F. A. Harrison, J. Phys. B **20**, 5865 (1987).
[24] R. J. Carman, IEEE J. Quantum Electron. **26**, 1588 (1990).
[25] M. Jogwich, B. A. Huber, and K. Wiesemann, Z. Phys. D **17**, 171 (1990).
[26] G. M. Petrov and C. M. Ferreira, Phys. Rev. E **59**, 3571 (1999).
[27] L. M. Biberman, V. S. Vorob'ev, and I. T. Iakubov, *Kinetics of Non-equilibrium Low-temperature Plasmas* (Plenum, New York, 1987).
[28] J. A. Hornbeck and J. P. Molnar, Phys. Rev. **84**, 621 (1951).
[29] D. Morris, Proc. Phys. Soc. London, Sect. A **68**, 11 (1955).
[30] M. Pahl, Z. Naturforsch. A **14a**, 239 (1959).
[31] J. S. Dahler, J. L. Franklin, M. S. B. Munson, and F. H. Field, J. Chem. Phys. **36**, 332 (1962).
[32] P. F. Knewstubb and A. W. Tickner, J. Chem. Phys. **36**, 674 (1962).
[33] P. M. Becker and F. W. Lampe, J. Am. Chem. Soc. **86**, 5347 (1964).
[34] P. M. Becker and F. W. Lampe, J. Chem. Phys. **42**, 3857 (1965).
[35] R. E. Huffmann and D. H. Katayama, J. Chem. Phys. **45**, 138 (1966).
[36] T. L. Rose, D. H. Katayama, J. A. Welsh, and J. F. Paulson, J. Chem. Phys. **70**, 4542 (1979).
[37] K. Stephan and T. D. Märk, Phys. Rev. A **32**, 1447 (1985).
[38] N. B. Kolokolov and A. B. Blagoev, Phys. Usp. **36**, 152 (1993).
[39] D. Smith and P. R. Cromey, J. Phys. B **1**, 638 (1968).
[40] J. C. Cronin and M. C. Sexton, J. Phys. B **1**, 889 (1968).
[41] A. K. Bhattacharya, J. Appl. Phys. **41**, 1707 (1970).
[42] B. H. Mahan, J. Chem. Phys. **43**, 3080 (1965).
[43] B. M. Smirnov, Sov. Phys. JETP **24**, 1180 (1967).
[44] R. Johnsen, A. Chen, and M. A. Biondi, J. Chem. Phys. **73**, 1717 (1980).
[45] M. Grössl, M. Langenwalter, H. Helm, and T. D. Märk, J. Chem. Phys. **74**, 1728 (1981).
[46] S. Yueh-Jaw and M. A. Biondi, Phys. Rev. A **17**, 868 (1978).
[47] C. C. Jen, Phys. Rev. **17**, 245 (1969).
[48] F. J. Mehr and M. A. Biondi, Phys. Rev. **16**, 322 (1968).
[49] T. F. O'Malley, A. J. Cunningham, and R. M. Hobson, J. Phys. B **5**, 2126 (1972).
[50] H. K. Gummel, IEEE Trans. Electron Devices **11**, 455 (1964).
[51] D. L. Scharfetter and H. K. Gummel, IEEE Trans. Electron Devices **16**, 64 (1969).
[52] H. D. Hagstrum, Phys. Rev. **96**, 325 (1954).
[53] A. Bogaerts, Ph.D. dissertation, University of Antwerp, 1996.
[54] A. Bogaerts and R. Gijbels, Plasma Phys. Rep. **24**, 573 (1998).
[55] A. V. Phelps, J. Phys. Chem. Ref. Data **20**, 557 (1991).
[56] G. Petrov, private communication.